



*Supplement of*

**Assimilation of carbonyl sulfide (COS) fluxes within the adjoint-based data assimilation system – Nanjing University Carbon Assimilation System (NUCAS v1.0)**

**Huajie Zhu et al.**

*Correspondence to:* Mousong Wu (mousongwu@nju.edu.cn)

The copyright of individual parts of the supplement might differ from the article licence.

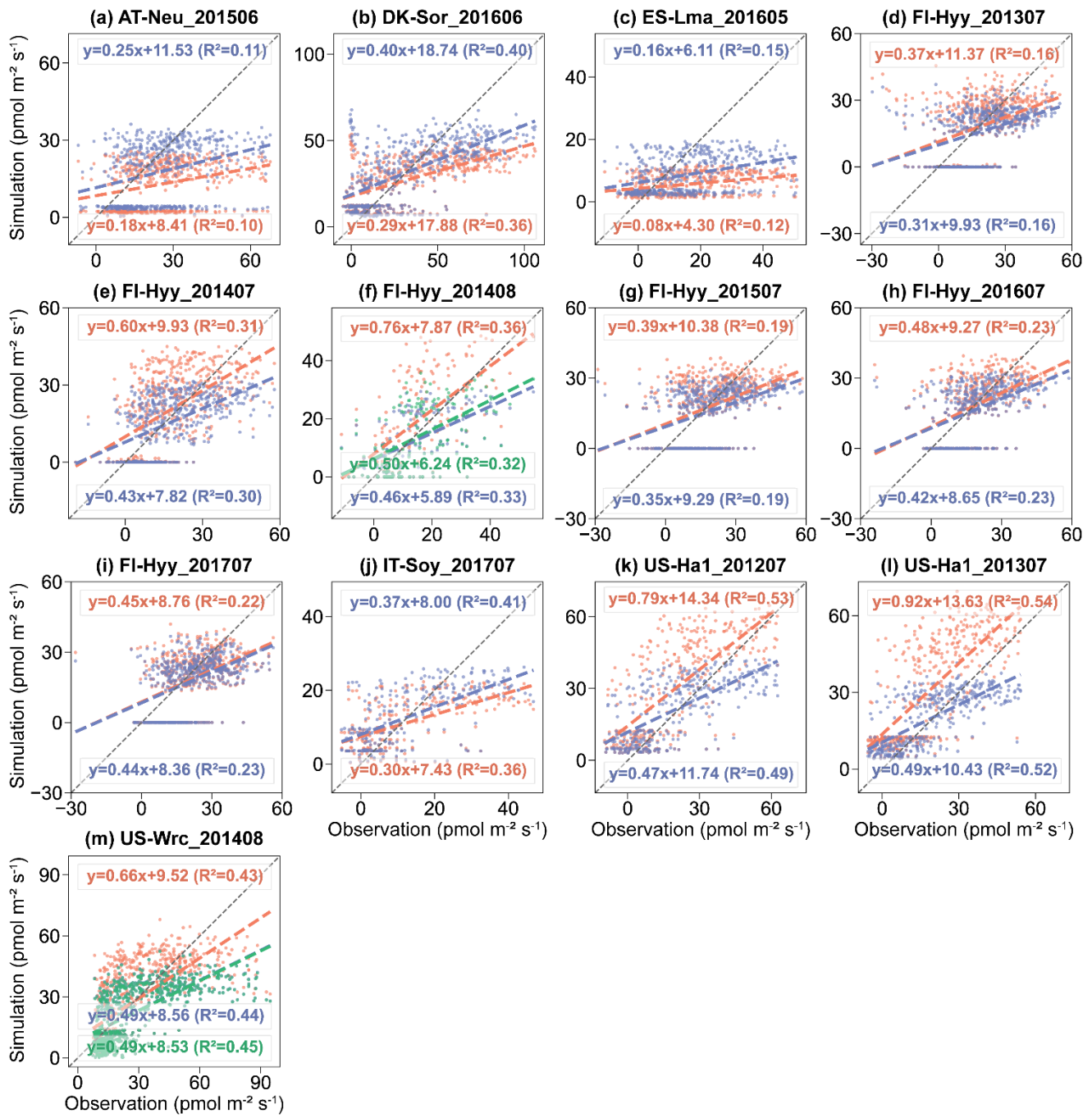


**Figure S1.** Scatterplots of observed versus simulated hourly COS flux using prior (red), single-site (blue) and two-site (green) posterior parameters.

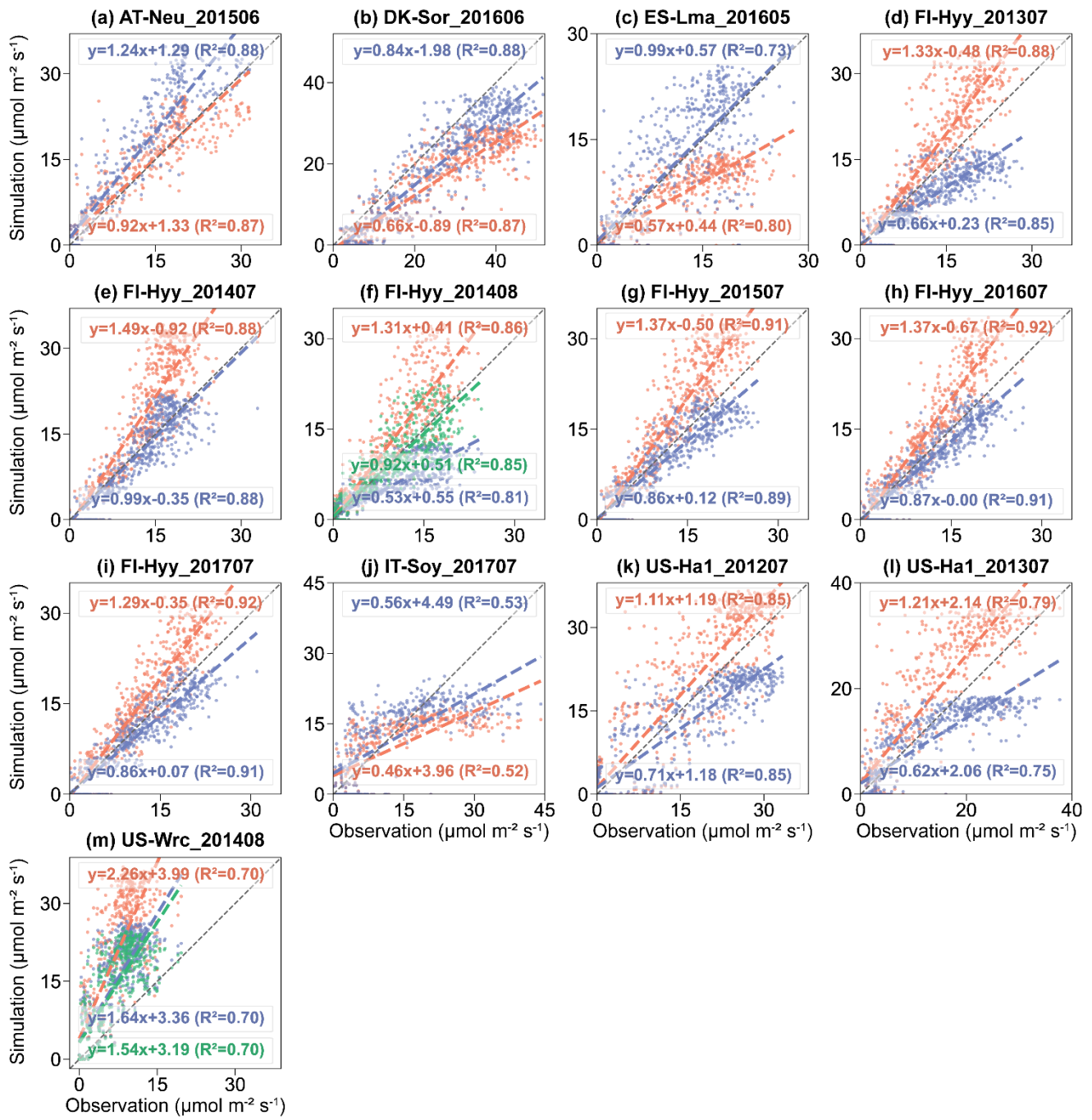


**Figure S2.** Scatterplots of observed versus simulated hourly GPP using prior (red), single-site (blue) and two-site (green) posterior parameters.

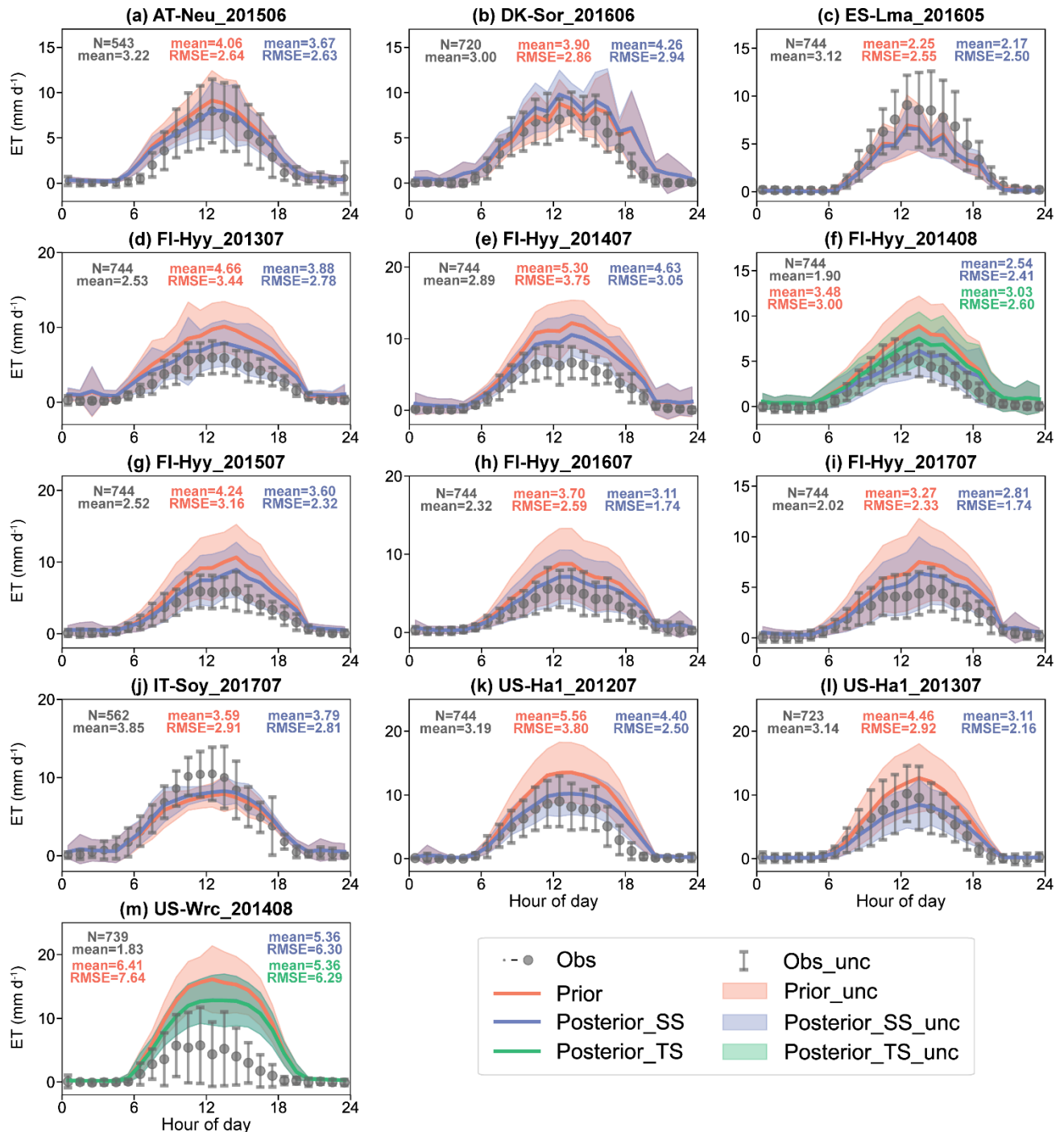


**Figure S3.** The diurnal cycle of observed (grey) and simulated ET using prior parameters (red), single-site (blue) and two-site (green) posterior parameters. The size of the circle indicates the number of observations within each circle (ranging from 1 to 31), and the error bars depict the standard deviations in the mean of observations from the variability within each circle. Lines connect the mean values of simulations, and pale bands depict the standard deviation in the mean of simulations from the variability within each bin.

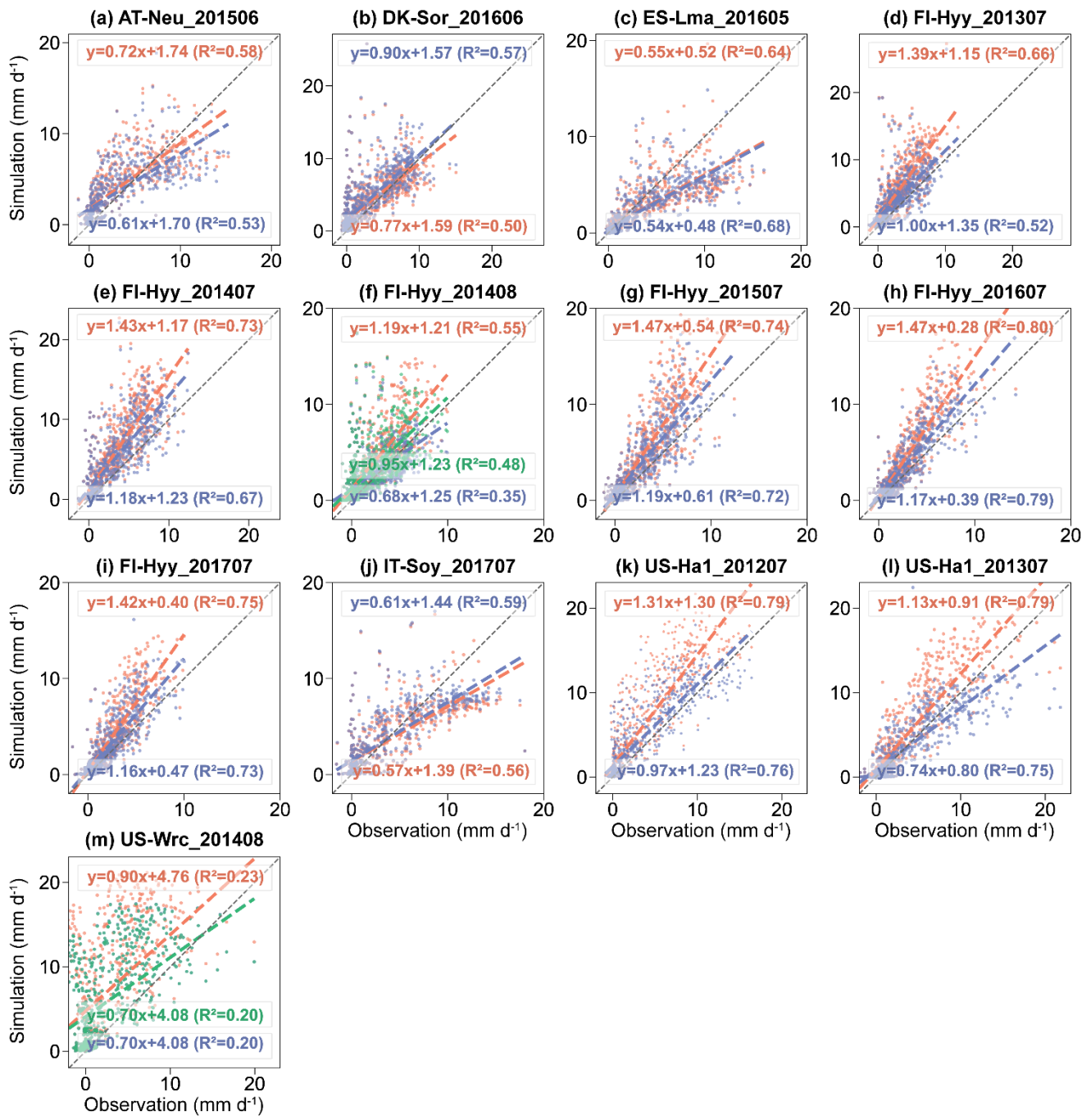


**Figure S4.** Scatterplots of observed versus simulated hourly ET using prior (red), single-site (blue) and two-site (green) posterior parameters.

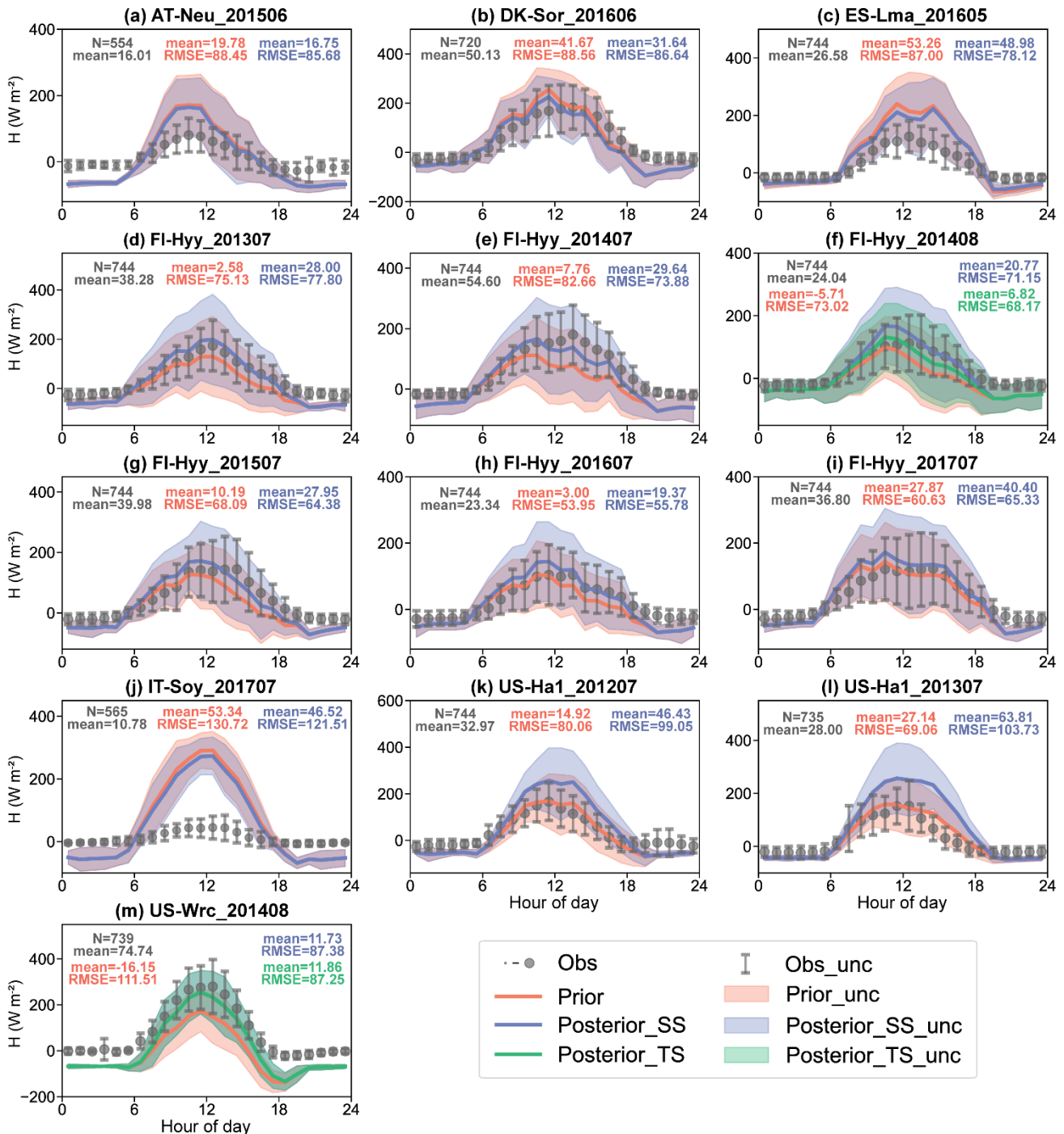


**Figure S5.** The diurnal cycle of observed (grey) and simulated  $H$  using prior parameters (red), single-site (blue) and two-site (green) posterior parameters. The size of the circle indicates the number of observations within each circle (ranging from 1 to 31), and the error bars depict the standard deviations in the mean of observations from the variability within each circle. Lines connect the mean values of simulations, and pale bands depict the standard deviation in the mean of simulations from the variability within each bin.

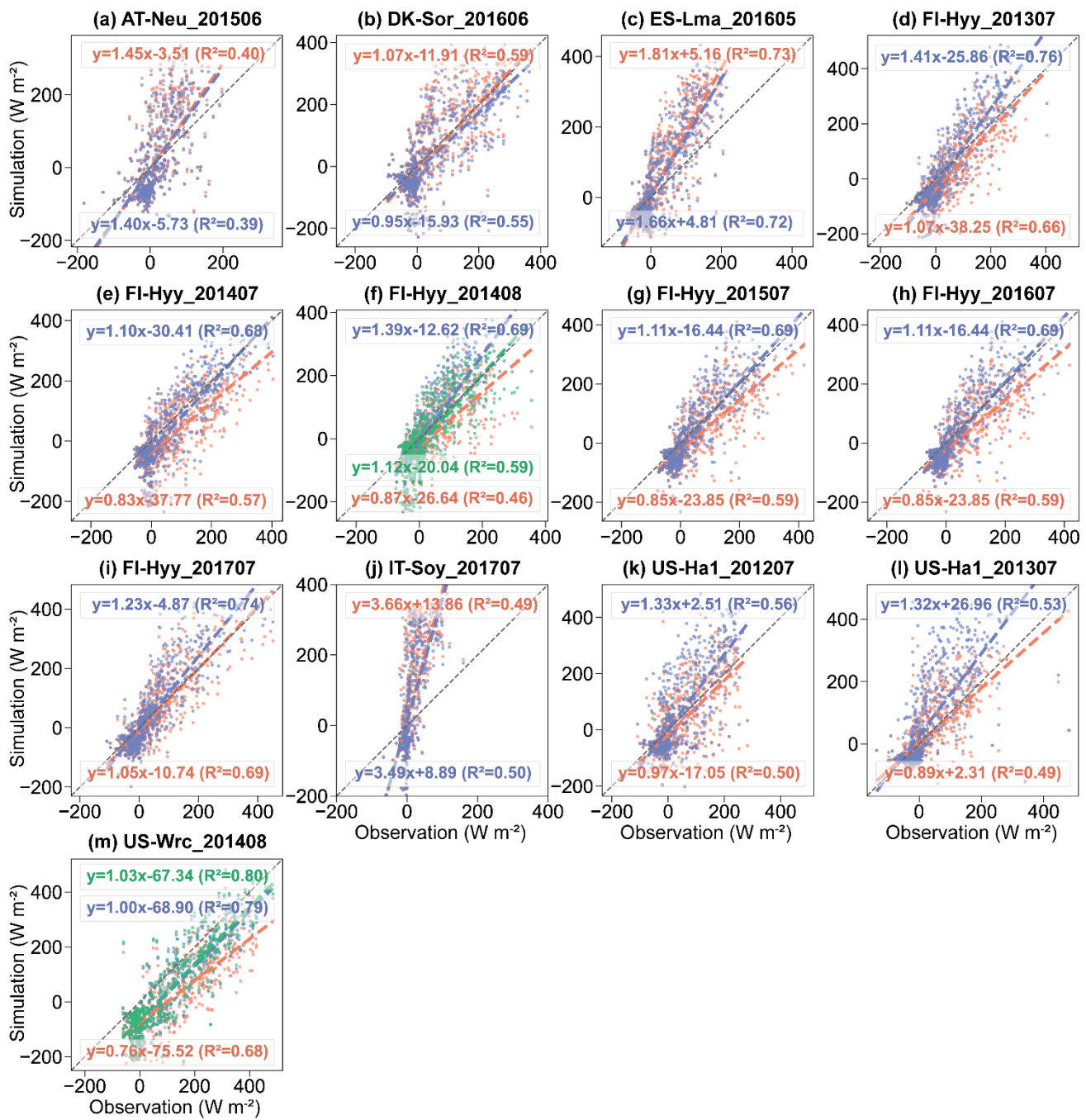


**Figure S6.** Scatterplots of observed versus simulated hourly H using prior (red), single-site (blue) and two-site (green) posterior parameters.

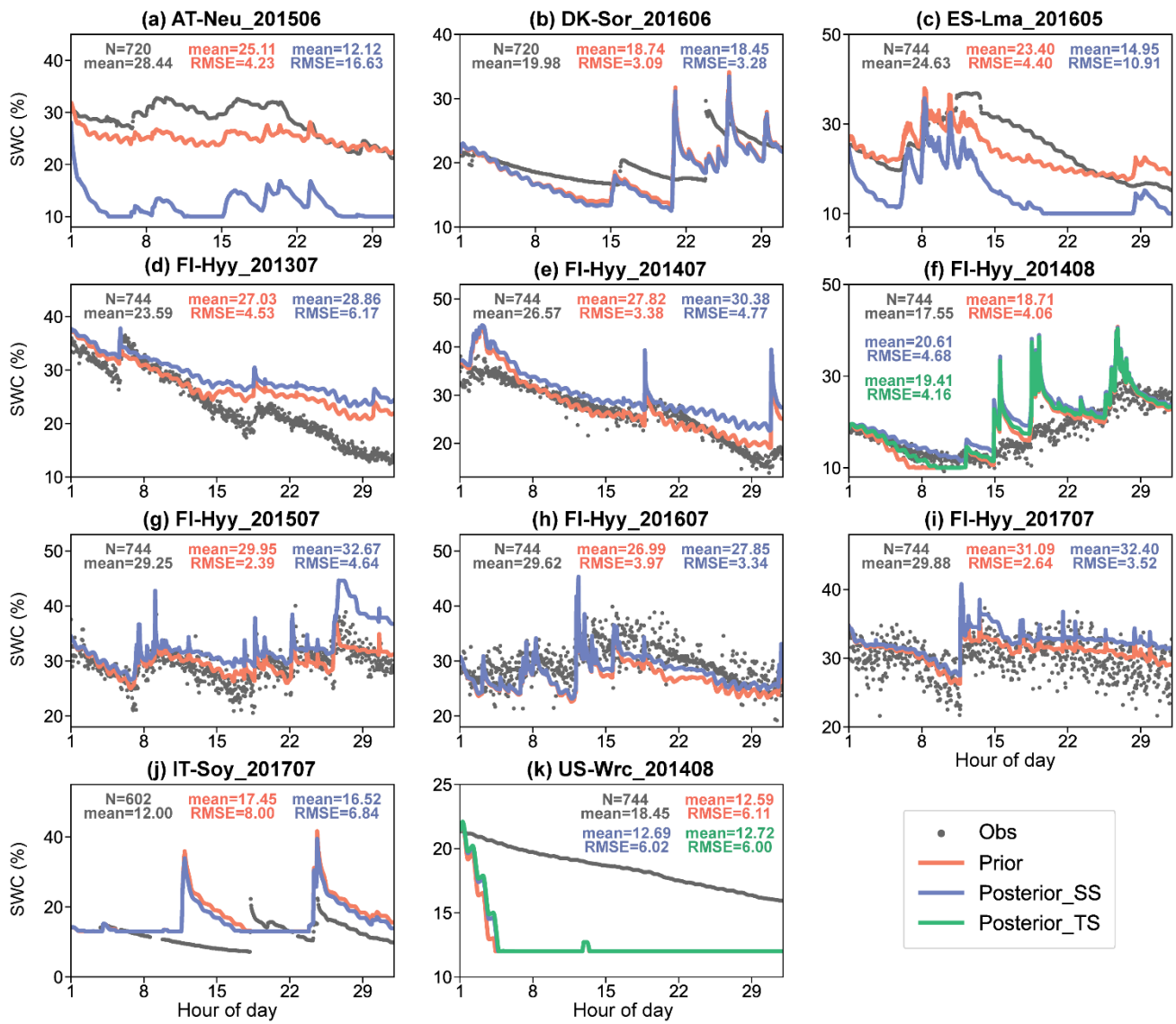


**Figure S7.** Observed (grey point) and simulated SWC (%). Results show SWC simulated using prior parameters (red line), single-site (blue line) and two-site (green line) posterior parameters.

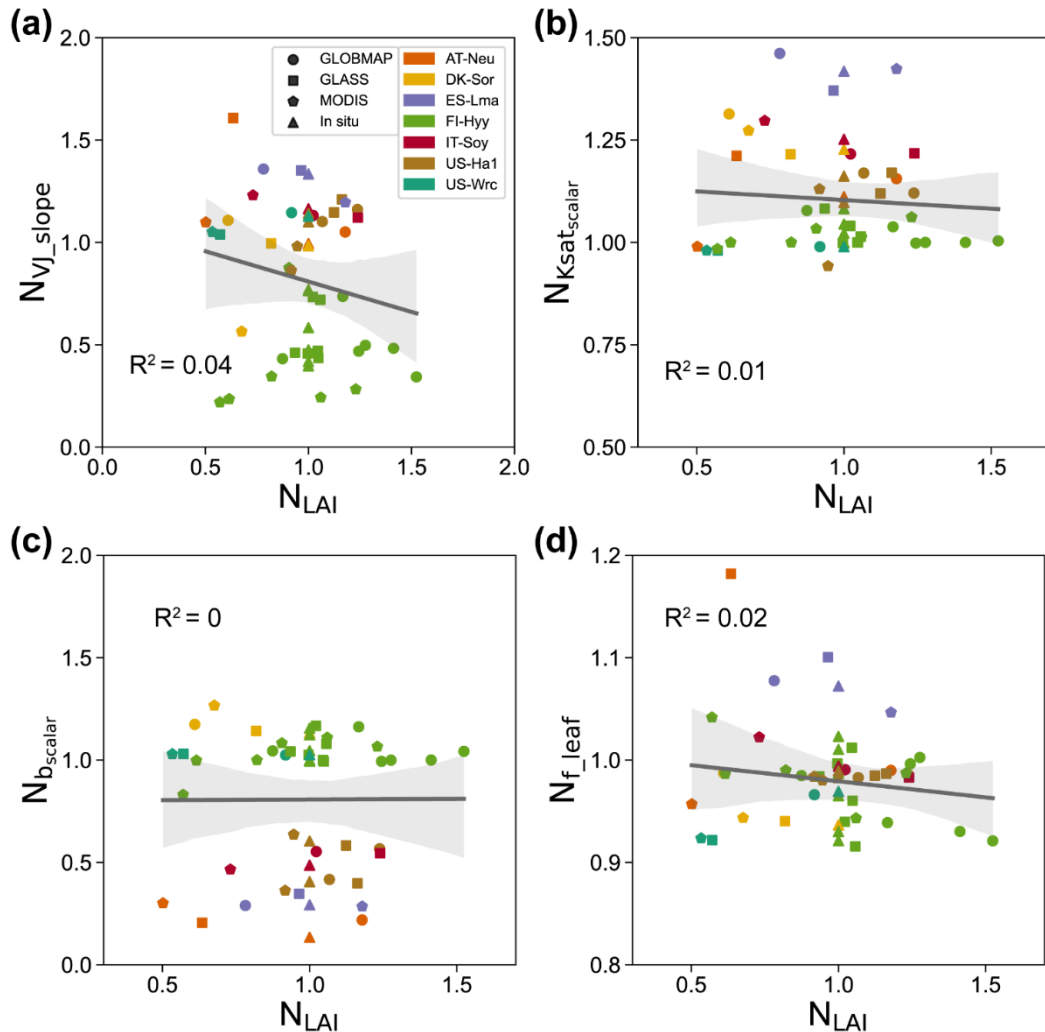


**Figure S8.** Influence of LAI on the posterior  $VJ_{slope}$ ,  $Ksat_{scalar}$ ,  $b_{scalar}$  and  $f_{leaf}$  obtained by the single-site experiments conducted at seven sites and driven by four LAI data (GLOBMAP, GLASS, MODIS and *in situ*). The posterior  $VJ_{slope}$ ,  $Ksat_{scalar}$ ,  $b_{scalar}$ ,  $f_{leaf}$  and the LAI were represented by their normalized values  $N_{VJ\_slope}$ ,  $N_{Ksat_{scalar}}$ ,  $N_{b_{scalar}}$ ,  $N_{f_{leaf}}$  and  $N_{LAI}$ , respectively. The posterior parameters were normalized by their prior values and the LAI were normalized by the *in situ* values. The linear regression fit line of the posterior parameters obtained based on the satellite-derived LAI (GLOBMAP, GLASS and MODIS) with the corresponding LAI data is shown, with 95% confidence interval spread around the line.

**Table S1.** PFT and Soil Texture descriptions in BEPS model.

| PFT No. | Descriptions                |
|---------|-----------------------------|
| 1       | Evergreen needleleaf forest |
| 2       | Deciduous needleleaf forest |
| 3       | Deciduous broadleaf forest  |
| 4       | Evergreen broadleaf forest  |

|                  |                      |
|------------------|----------------------|
| 5                | Mixed forest         |
| 6                | Shrub                |
| 7                | C <sub>3</sub> grass |
| 8                | C <sub>3</sub> crop  |
| 9                | C <sub>4</sub> grass |
| 10               | C <sub>4</sub> crop  |
| <hr/>            |                      |
| Soil texture No. | Description          |
| 1                | Sand                 |
| 2                | Loamy sand           |
| 3                | Sandy loam           |
| 4                | Loam                 |
| 5                | Silt loam            |
| 6                | Sandy clay loam      |
| 7                | Clay loam            |
| 8                | Silty clay loam      |
| 9                | Sandy clay           |
| 10               | Silty clay           |
| 11               | Clay                 |

**Table S2.** *alpha* and *beta* parameters for COS abiotic flux term.

| Site name | PFT in BEPS                 | PFT in (Whelan et al., 2016) | <i>alpha</i> (unitless) | <i>beta</i> (°C <sup>-1</sup> ) |
|-----------|-----------------------------|------------------------------|-------------------------|---------------------------------|
| AT-Neu    | C <sub>3</sub> grass        | Savanna                      | -9.54                   | 0.108                           |
| ES-Lma    | C <sub>3</sub> grass        | Savanna                      | -9.54                   | 0.108                           |
| DK-Sor    | Deciduous broadleaf forest  | Temperate forest             | -7.77                   | 0.119                           |
| US-Ha1    | Deciduous broadleaf forest  | Temperate forest             | -7.77                   | 0.119                           |
| FI-Hyy    | Evergreen needleleaf forest | Temperate forest             | -7.77                   | 0.119                           |
| US-Wrc    | Evergreen needleleaf forest | Temperate forest             | -7.77                   | 0.119                           |
| IT-Soy    | C <sub>3</sub> crop         | Soy field                    | -6.12                   | 0.096                           |

**Table S3.** Parameters for COS biotic flux term.

| PFT in BEPS          | PFT in (Whelan et al., 2022) | SWC <sub>opt</sub> (%) | F <sub>opt</sub> ( pmol m <sup>-2</sup> s <sup>-1</sup> ) with temperature (°C) at SWC <sub>opt</sub>            | SWC <sub>g</sub> (%) | F <sub>opt</sub> ( pmol m <sup>-2</sup> s <sup>-1</sup> ) with temperature (°C) at SWC <sub>g</sub>              |
|----------------------|------------------------------|------------------------|--|----------------------|--|
| C <sub>3</sub> grass | Grassland                    | 12.5                   | F <sub>opt</sub> : -4.5<br>F <sub>T<sub>g</sub></sub> : -1.5<br>T <sub>opt</sub> : -10.9<br>T <sub>g</sub> : -25 | 26.9                 | F <sub>opt</sub> : -2.3<br>F <sub>T<sub>g</sub></sub> : -1.3<br>T <sub>opt</sub> : -14.8<br>T <sub>g</sub> : -25 |

|                             |                                 |      |  |      |  |
|-----------------------------|---------------------------------|------|--|------|--|
| Deciduous broadleaf forest  | Forest - Temperate or broadleaf | 24.6 | 12.6   | 51   | -0.18T+0.48  |
| Evergreen needleleaf forest | Forest – Boreal or needleleaf   | 12.5 | $F_{opt}$ : -18<br>$F_{T_g}$ : -12<br>$T_{opt}$ : 28<br>$T_g$ : 35 | 19.3 | $F_{opt}$ : -5.9<br>$F_{T_g}$ : -3.8<br>$T_{opt}$ : 28<br>$T_g$ : 35 |
| C <sub>3</sub> crop         | Agricultural                    | 17.7 | -9.7   | 22   | -5.36  |

**Table S4.** Description of parameters used for optimizations within the Nanjing University Carbon Assimilation System (NUCAS). Parameters are either specified per PFT, per soil texture, or globally, i.e., all PFTs and textures share one value, as indicated in column 3.

| No. | Parameter    | Dependent | Unit                                 | Description  | Prior Value | Prior Uncertainty |
|-----|--------------|-----------|--------------------------------------|--|-------------|-------------------|
| 1   |              |           |                                      |  | 62.5        | 15.625            |
| 2   |              |           |                                      |  | 39.1        | 9.775             |
| 3   |              |           |                                      |  | 57.7        | 14.425            |
| 4   |              |           |                                      |  | 29          | 7.25              |
| 5   | $V_{cmax25}$ | PFT       | $\mu\text{mol m}^{-2} \text{s}^{-1}$ | Maximum carboxylation rate of Rubisco at 25°C  | 66          | 16.5              |
| 6   |              |           |                                      |  | 57.85       | 14.4625           |
| 7   |              |           |                                      |  | 48          | 12                |
| 8   |              |           |                                      |  | 84.5        | 21.125            |
| 9   |              |           |                                      |  | 30          | 7.5               |
| 10  |              |           |                                      |  | 30          | 7.5               |
| 11  |              |           |                                      |  | 2.39        | 0.5975            |
| 12  |              |           |                                      |  | 2.39        | 0.5975            |
| 13  |              |           |                                      |  | 2.39        | 0.5975            |
| 14  |              |           |                                      |  | 2.39        | 0.5975            |
| 15  | VJ_slope     | PFT       | unitless                             | Slope of the $V_{cmax}$ and $J_{max}$ (maximum electron transport rate) relationship | 2.39        | 0.5975            |
| 16  |              |           |                                      |  | 2.39        | 0.5975            |
| 17  |              |           |                                      |  | 2.39        | 0.5975            |
| 18  |              |           |                                      |  | 2.39        | 0.5975            |
| 19  |              |           |                                      |  | 2.39        | 0.5975            |
| 20  |              |           |                                      |  | 2.39        | 0.5975            |
| 21  |              |           |                                      |  | 0.046       | 0.0115            |
| 22  |              |           |                                      |  | 0.046       | 0.0115            |
| 23  |              |           |                                      |  | 0.046       | 0.0115            |
| 24  | Q10          | PFT       | unitless                             | Soil respiration temperature factor  | 0.046       | 0.0115            |
| 25  |              |           |                                      |  | 0.046       | 0.0115            |
| 26  |              |           |                                      |  | 0.046       | 0.0115            |
| 27  |              |           |                                      |  | 0.046       | 0.0115            |
| 28  |              |           |                                      |  | 0.046       | 0.0115            |

|    |                        |         |                   |  |          |
|----|------------------------|---------|-------------------|--|----------|
| 29 |                        |         |                   | 0.046  | 0.0115   |
| 30 |                        |         |                   | 0.046  | 0.0115   |
| 31 |                        |         |                   | 6.2473   | 1.561825 |
| 32 |                        |         |                   | 6.2473   | 1.561825 |
| 33 |                        |         |                   | 6.2473   | 1.561825 |
| 34 |                        |         |                   | 6.2473   | 1.561825 |
| 35 | SIF_alpha              | PFT     | W m <sup>-2</sup> | Quadratic term coefficient for the relationship between additional heat dissipation under light adapted conditions and relative reduction of photochemical yield | 6.2473   |
| 36 |                        |         |                   |  | 1.561825 |
| 37 |                        |         |                   | 6.2473   | 1.561825 |
| 38 |                        |         |                   | 6.2473   | 1.561825 |
| 39 |                        |         |                   | 6.2473   | 1.561825 |
| 40 |                        |         |                   | 6.2473   | 1.561825 |
| 41 |                        |         |                   | 0.5994   | 0.14985  |
| 42 |                        |         |                   | 0.5994   | 0.14985  |
| 43 |                        |         |                   | 0.5994   | 0.14985  |
| 44 |                        |         |                   | 0.5994   | 0.14985  |
| 45 | SIF_beta               | PFT     | W m <sup>-2</sup> | Primary term coefficient for the relationship between additional heat dissipation under light adapted conditions and relative reduction of photochemical yield   | 0.5994   |
| 46 |                        |         |                   |  | 0.14985  |
| 47 |                        |         |                   | 0.5994   | 0.14985  |
| 48 |                        |         |                   | 0.5994   | 0.14985  |
| 49 |                        |         |                   | 0.5994   | 0.14985  |
| 50 |                        |         |                   | 0.5994   | 0.14985  |
| 51 |                        |         |                   | 1  | 0.25     |
| 52 |                        |         |                   | 1  | 0.25     |
| 53 |                        |         |                   | 1  | 0.25     |
| 54 |                        |         |                   | 1  | 0.25     |
| 55 |                        |         |                   | 1  | 0.25     |
| 56 | Ksat <sub>scalar</sub> | texture | unitless          | Scaling factor of saturated hydraulic conductivity (Ksat)  | 1        |
| 57 |                        |         |                   |  | 0.25     |
| 58 |                        |         |                   | 1  | 0.25     |
| 59 |                        |         |                   | 1  | 0.25     |
| 60 |                        |         |                   | 1  | 0.25     |
| 61 |                        |         |                   | 1  | 0.25     |
| 62 |                        |         |                   | 1  | 0.25     |
| 63 |                        |         |                   | 1  | 0.25     |
| 64 |                        |         |                   | 1  | 0.25     |
| 65 | b <sub>scalar</sub>    | texture | unitless          | Scaling factor of Campbell parameter b (the exponential parameter of Campbell's soil moisture retention model)   | 1        |
| 66 |                        |         |                   |  | 0.25     |
| 67 |                        |         |                   | 1  | 0.25     |
| 68 |                        |         |                   | 1  | 0.25     |
| 69 |                        |         |                   | 1  | 0.25     |

|    |        |        |          |  |  |         |        |      |
|----|--------|--------|----------|--|--|---------|--------|------|
| 70 |        |        |          |  |  |         | 1      | 0.25 |
| 71 |        |        |          |  |  |         | 1      | 0.25 |
| 72 |        |        |          |  |  |         | 1      | 0.25 |
| 73 | f_leaf | global | unitless | The ratio of photosynthetically active radiation to shortwave radiation  |  | 0.466   | 0.033  |      |
| 74 | kc25   | global | μbar     | Michaelis–Menten constants for CO <sub>2</sub> in 25 °C  |  | 274.6   | 68.65  |      |
| 75 | ko25   | global | mbar     | Michaelis–Menten constants for O <sub>2</sub> in 25 °C   |  | 419.8   | 104.95 |      |
| 76 | tau25  | global | unitless | The CO <sub>2</sub> /O <sub>2</sub> specificity factor, which reflects the carbon assimilation efficiency of Rubisco |  | 2904.12 | 726.03 |      |

**Table S5.** Summary of configurations of twin experiments.  $J_{initial}$  and  $J_{final}$  denote the initial value and the final value of the cost function  $J(x)$  respectively;  $G_{initial}$  and  $G_{final}$  denote the initial value and the final value of the gradient respectively;  $D_{initial}$  and  $D_{final}$  denote the initial value and the final value of the distance ( $D_x$ ) between the parameter vector and the prior parameter vector. The initial value ( $D_{initial}$ ) of  $D_x$  for all twin experiments is 7.48, due to an identical perturbation size (0.2) being applied. The suffix “\*\*” indicates the two-site experiment.

| Site name | Data duration | $J_{initial}$ | $J_{final}$ | $G_{initial}$ | $G_{final}$ | $D_{final}$ | Relative changes of parameters (%) |           |                  |              |           |
|-----------|---------------|---------------|-------------|---------------|-------------|-------------|------------------------------------|-----------|------------------|--------------|-----------|
|           |               |               |             |               |             |             | $V_{cmax25}$                       | VJ_slope  | $K_{sat,scalar}$ | $b_{scalar}$ | f_leaf    |
| AT-Neu    | June 2015     | 55.08         | 6.52E-16    | 48.09         | 6.65E-07    | 3.14E-08    | -8.13E-10                          | -3.16E-09 | -6.88E-10        | -1.68E-09    | 1.24E-09  |
| DK-Sor    | June 2016     | 77.13         | 7.45E-16    | 77.01         | 1.30E-06    | 3.56E-08    | 1.55E-09                           | -8.85E-10 | -2.82E-09        | -1.08E-09    | -1.80E-09 |
| ES-Lma    | May 2016      | 53.01         | 3.34E-15    | 51.59         | 1.55E-06    | 6.60E-08    | -1.06E-09                          | 1.88E-09  | 8.54E-09         | 7.58E-09     | 4.26E-11  |
| FI-Hyy    | July 2013     | 73.44         | 2.02E-17    | 70.43         | 1.10E-06    | 3.68E-09    | 1.29E-10                           | 3.66E-10  | -9.30E-11        | 4.46E-10     | -2.01E-10 |
|           | July 2014     | 77.59         | 1.06E-17    | 76.83         | 2.97E-07    | 4.02E-09    | 3.18E-10                           | -6.80E-10 | -2.08E-11        | -1.96E-10    | -1.56E-10 |
|           | August 2014   | 74.09         | 9.27E-18    | 70.00         | 4.63E-07    | 4.05E-09    | -7.33E-11                          | 1.22E-10  | 5.99E-10         | 4.59E-10     | 2.20E-10  |
|           | July 2015     | 72.76         | 1.19E-16    | 70.07         | 7.93E-07    | 1.50E-08    | -1.16E-10                          | -4.87E-10 | 1.14E-11         | 7.20E-10     | 1.07E-09  |
|           | July 2016     | 75.89         | 1.13E-18    | 73.35         | 2.12E-07    | 9.30E-10    | -9.64E-11                          | 1.08E-10  | 3.16E-11         | 3.95E-11     | -5.55E-12 |
|           | July 2017     | 73.94         | 8.47E-17    | 73.64         | 7.18E-07    | 1.24E-08    | 8.68E-11                           | 7.31E-10  | 3.69E-12         | 2.01E-10     | 8.47E-10  |
| IT-Soy    | July 2017     | 50.75         | 5.09E-13    | 38.82         | 4.94E-07    | 4.19E-08    | 2.86E-09                           | -7.41E-09 | 2.74E-09         | -5.89E-09    | -5.70E-10 |
| US-Ha1    | July 2012     | 66.15         | 1.93E-19    | 59.66         | 2.05E-07    | 5.87E-10    | -6.01E-12                          | 7.29E-11  | 1.35E-11         | 7.87E-11     | -5.81E-12 |
|           | July 2013     | 66.50         | 1.61E-17    | 60.25         | 9.99E-07    | 4.42E-09    | 4.42E-09                           | 7.44E-10  | -9.77E-11        | 4.07E-10     | -3.52E-11 |
| US-Wrc    | August 2014   | 58.97         | 3.28E-18    | 46.87         | 1.45E-07    | 2.14E-09    | -1.16E-10                          | 4.40E-10  | 1.22E-10         | -7.50E-11    | 6.04E-11  |
| FI-Hyy*   | August 2014   | 108.04        | 3.95E-15    | 119.27        | 1.28E-06    | 1.92E-08    | -1.98E-11                          | 1.52E-10  | -2.57E-10        | -7.38E-10    | 1.41E-09  |
|           | US-Wrc*       |               |             |               |             |             |                                    |           | -3.41E-10        | 4.63E-10     |           |

## References

- Whelan, M. E., Hilton, T. W., Berry, J. A., Berkelhammer, M., Desai, A. R., and Campbell, J. E.: Carbonyl sulfide exchange in soils for better estimates of ecosystem carbon uptake, *Atmos. Chem. Phys.*, 16, 3711–3726, <https://doi.org/10.5194/acp-16-3711-2016>, 2016.
- Whelan, M. E., Shi, M., Sun, W., Vries, L. K.-d., Seibt, U., and Maseyk, K.: Soil Carbonyl Sulfide (OCS) Fluxes in Terrestrial Ecosystems: An Empirical Model, *Journal of Geophysical Research: Biogeosciences*, 127, e2022JG006858, <https://doi.org/10.1029/2022JG006858>, 2022.